

RESEARCH ARTICLE

Characterization of Liver Monocytic Myeloid-Derived Suppressor Cells and Their Role in a Murine Model of Non-Alcoholic Fatty Liver Disease

Liyang Yao¹, Masanori Abe^{1*}, Keitarou Kawasaki¹, Sheikh Mohammad Fazle Akbar², Bunzo Matsuura¹, Morikazu Onji³, Yoichi Hiasa¹

1 Department of Gastroenterology and Metabology, Ehime University Graduate School of Medicine, To-on, Ehime, Japan, **2** Department of Medical Sciences, Toshiba General Hospital, Shinagawa, Tokyo, Japan, **3** Department of Internal Medicine, Imabari Saiseikai Medical-Welfare Center, Imabari, Ehime, Japan

* masaben@m.ehime-u.ac.jp



OPEN ACCESS

Citation: Yao L, Abe M, Kawasaki K, Akbar SMF, Matsuura B, Onji M, et al. (2016) Characterization of Liver Monocytic Myeloid-Derived Suppressor Cells and Their Role in a Murine Model of Non-Alcoholic Fatty Liver Disease. PLoS ONE 11(2): e0149948. doi:10.1371/journal.pone.0149948

Editor: Li Yang, National Cancer Institute, UNITED STATES

Received: December 6, 2015

Accepted: February 8, 2016

Published: February 22, 2016

Copyright: © 2016 Yao et al. This is an open access article distributed under the terms of the [Creative Commons Attribution License](https://creativecommons.org/licenses/by/4.0/), which permits unrestricted use, distribution, and reproduction in any medium, provided the original author and source are credited.

Data Availability Statement: All relevant data are within the paper and its Supporting Information file.

Funding: This work was supported in part by Grants-in-Aid for Scientific Research (JSPS KAKENHI 15K09007 to MA and 15K09006 to YH) from the Japanese Ministry of Education, Culture, Sports, Science and Technology, as well as a Grant-in-Aid for Scientific Research and Development from the Japanese Ministry of Health, Labor and Welfare (to MA and YH). The funders had no role in study design, data collection and analysis, decision to publish, or preparation of the manuscript.

Abstract

Myeloid-derived suppressor cells (MDSCs) are potent suppressors of T cell immunity in tumors and inflammatory diseases. They are identified by surface expression of CD11b⁺Gr1⁺ in mice, and CD11b⁺Gr1⁺ cells accumulate in the livers of obese mice. However, many myeloid cells share these CD11b⁺Gr1⁺ markers. Accordingly, the aim of this study was to identify the authentic phenotype of MDSCs and investigate their functions in non-alcoholic fatty liver disease (NAFLD). C57BL/6J mice were divided into 2 diet groups: a normal control group and high-fat group to induce NAFLD. We demonstrated that monocytic CD11b⁺Gr1^{dim} cells could be further divided into 2 populations based on side scatter (SSC) during flow cytometry. We found that SSC^{low}CD11b⁺Gr1^{dim} cells accumulated in the livers of NAFLD mice over time, and that these cells were recruited by the chemokine CCL2 and its receptor CCR2 and might expand in the liver via macrophage colony-stimulating factor stimulation. Furthermore, SSC^{low}CD11b⁺Gr1^{dim} cells had a strong suppressive ability on T cells; this effect was not observed for SSC^{high}CD11b⁺Gr1^{dim} cells, and was dependent on nitric oxide production by inducible nitric oxide synthase. Our findings demonstrate that SSC^{low}CD11b⁺Gr1^{dim} cells represent authentic MDSCs in NAFLD livers, and might serve an important negative feedback function in liver inflammation.

Introduction

Non-alcoholic fatty liver disease (NAFLD) is currently one of the most commonly diagnosed liver diseases worldwide, and includes a wide spectrum of liver pathologies, including simple steatosis, steatohepatitis, liver fibrosis, and cirrhosis [1, 2]. Altered immunomodulation is thought to contribute to the pathogenesis of NAFLD [3]; the T cell-mediated immune response is considered to play a critical role in the associated liver injury [4]. It has been observed that

Competing Interests: The authors have declared that no competing interests exist.

the number of CD4⁺CD25⁺ Treg cells is reduced in obese livers, which leads to impaired suppression of inflammatory responses [5]. M2 macrophages, also categorized as immunosuppressive cells, play a role in limiting liver inflammation and injury in NAFLD [6].

Myeloid-derived suppressor cells (MDSCs) are a heterogeneous population of immature myeloid cells and comprise myeloid precursors of granulocytes, macrophages, and dendritic cells. They accumulate in tumor-bearing hosts, trauma sites, and infections to suppress immune responses via arginase-1, inducible nitric oxide synthase (iNOS), or reactive oxygen species (ROS). In mice, MDSCs were originally defined as CD11b⁺Gr1⁺ cells, whereas in humans, these cells are mainly defined as CD11b⁺CD33⁺CD15⁺HLA-DR⁻ or CD11b⁺CD33⁺CD14⁺HLA-DR^{-/low} cells [7, 8]. However, a specific marker for MDSCs has not yet been described because other myeloid cells share their surface molecules, such as neutrophils, monocytes, and myeloid dendritic cells. Therefore, the most reliable feature that can be used to distinguish MDSCs from other myeloid cells appears to be their suppressive function.

Some studies have indicated that MDSCs play a role in hepatocellular carcinoma (HCC), hepatitis, or liver fibrosis both in patients and mouse models [9–13]. Recently, MDSCs have been found to accumulate in the livers of obese mice to suppress inflammation and maintain liver homeostasis; these MDSCs were identified as CD11b⁺Gr1⁺ [14, 15]. The Gr1 marker is a composite epitope between Ly6C and Ly6G antigens, and MDSCs can be further subdivided into Ly6C⁺ monocytic and Ly6G⁺ granulocytic MDSCs using these 2 antigens [12, 16]. However, other studies have reported that liver CD11b⁺Ly6C⁺ or CD11b⁺Gr1⁺ cells, categorized as macrophages, monocytes, or immature myeloid cells, contribute to liver inflammation [17–19], suggesting that the phenotype of liver MDSCs needs further investigation and specification.

In this study, we successfully elucidated the profile of authentic monocytic MDSCs that accumulated in the livers of NAFLD model mice and assess their function with respect to T cell suppression and their role in the pathogenesis of liver inflammation in NAFLD.

Materials and Methods

Mice

Five-week-old male C57BL/6J and C3H/HeN mice were purchased from CLEA Japan (Tokyo, Japan). After 1 week of acclimatization, C57BL/6J mice were divided into 2 groups. The control group was fed a normal diet (13% fat, 26% protein, and 60% carbohydrates; 360 kcal/100 g). The NAFLD group was fed a high-fat diet (60% fat, 20% protein, and 20% carbohydrates; 520 kcal/100 g; D12492; Research Diets, New Brunswick, NJ, USA). The mice were fed these diets for either 3 or 12 months. The NAFLD group fed the high-fat diet for 12 months showed more severe steatosis than those fed the high-fat diet for 3 months. All animals received humane care, and the study protocols were approved by the Institutional Animal Care and Use Committee of Ehime University (No. 05-TI-72-16). Following sacrifice, 10 mg of liver was harvested, submerged in RNA-later (Life Technologies, Carlsbad, CA, USA), and stored at -20°C. Some liver tissue samples were stored at -80°C.

Cell isolation

Liver non-parenchymal cells and splenocytes were prepared using the procedure described by Chen et al. [20]. T cells were isolated from C57BL/6J mouse splenocytes using the mouse Pan T Cell Isolation Kit II (Miltenyi Biotec, Bergisch Gladbach, Germany). Dendritic cells were isolated from C3H/HeN mouse splenocytes using mouse CD11c Microbeads (Miltenyi Biotec), using an autoMACS Pro Separator (Miltenyi Biotec).

Flow cytometry and cell sorting

Liver non-parenchymal cell suspensions were pre-incubated with anti-CD16/CD32 (clone 93) to block non-specific Fc γ binding, and then stained with mouse monoclonal antibodies (mAbs) against the following: CD45 (30-F11), Gr1 (RB6-8C5), CD11b (M1/70), Ly6G (1A8), Ly6C (AL-21), CD11c (HL3), CD80 (16-10A1), CD31 (MEC13.3), iNOS (6/iNOS/NOS Type II), and interferon (IFN)- γ (XMG 1.2) (all from BD Biosciences, San Jose, CA, USA), or F4/80 (BM8) (BioLegend, San Diego, CA, USA), CD115 (AFS98) (TONBO Biosciences, San Diego, CA, USA), CD274 (MIH6) (AbD Serotec, Kidlington, UK), and CCR2 (R&D Systems, Minneapolis, MN, USA). For intracellular cytokine staining, cells were lysed using a Fixation and Permeabilization Kit (Invitrogen, Carlsbad, CA, USA) based on the manufacturer's instructions. Flow cytometry was performed on a Becton Dickinson Fluorescence Activated Cell Sorter (FACS) Calibur using CellQuest Software (Becton Dickinson, Franklin Lakes, NJ, USA). Data were analyzed using FlowJo (Tree Star, Ashland, OR, USA). Liver non-parenchymal cells were stained with mAbs specific to CD11b and Gr1, and cell scatter (SSC)^{high}CD11b⁺Gr1^{dim} cells and SSC^{low}CD11b⁺Gr1^{dim} cells were sorted using the BD FACSAria™ Cell Sorting System (Becton Dickinson). The purity of all sorted cells was greater than 98%.

MDSC functional assay

To investigate the suppressive function of MDSCs, T cells were stained with 10 μ M 5-(and 6)-carboxy-fluorescein diacetate, succinimidyl ester (CFSE) according to the manufacturer's instructions (Molecular Probes, Carlsbad, CA, USA). CFSE-labeled T cells were cultured with Dynabeads Mouse T-Activator CD3/CD28 (Life Technologies) in the absence or presence of sorted SSC^{high}CD11b⁺Gr1^{dim} cells or SSC^{low}CD11b⁺Gr1^{dim} cells from the livers of NAFLD mice. After 60 h, T cell proliferation was analyzed by flow cytometry. Division indices were calculated using FlowJo software. To determine the roles of iNOS, ROS, and arginase 1 in T cell proliferation, 0.5 μ M L-N⁶-(1-iminoethyl) lysine dihydrochloride (L-NIL; Sigma-Aldrich, Gillingham, UK), 1000 U/mL catalase (Sigma-Aldrich), or 1 mM N-hydroxy-nor-arginine (nor-NOHA; Cayman Chemical, Ann Arbor, MI, USA), was added at the start of the cultures, respectively. In some experiments, T cells were stimulated with phorbol 12-myristate 13-acetate (50 ng/mL; Sigma) and ionomycin (1 μ g/mL; Sigma). Allogenic mixed lymphocyte reactions were used to confirm the suppressive ability of MDSCs. T cells from C57BL/6J mice were mixed with dendritic cells from C3H/HeN mice and co-cultured in the absence or presence of sorted SSC^{high}CD11b⁺Gr1^{dim} cells or SSC^{low}CD11b⁺Gr1^{dim} cells from the livers of NAFLD mice at different ratios. [³H]-thymidine (1.0 μ Ci/mL; Amersham Biosciences, Buckinghamshire, UK) was diluted in sterile RPMI-1640 and added to the cultures for the last 16 h. The stimulation index was calculated using a formula described previously [20]. All culturing was performed in 96-well U-bottomed plates (Corning Inc., New York, NY, USA).

Nitrite and CCL2 determination

The NO concentration in co-culture supernatants was measured using the Griess Reagent System (Promega, Madison, WI, USA) according to manufacturer's protocol. For CCL2 determination, protein was extracted from the liver lysate using RIPA buffer supplemented with protease inhibitor cocktail. CCL2 expression was investigated with a RayBio Mouse CCL2 ELISA Kit (RayBiotech, Norcross, GA, USA) according to the manufacturer's protocol.

In vitro MDSC migration assay

Isolated $SSC^{\text{low}}CD11b^+Gr1^{\text{dim}}$ cells from the livers of NAFLD mice were resuspended at 2×10^6 cells/mL in serum-free RPMI 1640 media. An aliquot of 150 μL of medium containing 0 ng/mL, 10 ng/mL, or 50 ng/mL murine recombinant chemokine ligand 2 (CCL2) (R&D) was added to the feeder tray. Then, an aliquot (100 μL) of the suspension was added to the membrane chamber of the CytoSelect™ 96-Well Cell Migration Assay (5 μm , Fluorometric Format; Cell Biolabs, San Diego, CA, USA). The kit was incubated at 37°C for 2 h in a 5% CO_2 cell culture incubator. Cells that had migrated were stained using CyQUANT GR dye, and fluorescence intensity was measured with a Flex Station 96 ED (Molecular Devices, Sunnyvale, CA, USA). Data are shown in relative fluorescence units.

Immunohistochemistry

Frozen liver tissues were fixed in neutral-buffered formalin, paraffin-embedded, and cut into 3- μm -thick sections. Sections were dewaxed and rehydrated, and antigens were retrieved by autoclaving for 1 min at 125°C in EDTA buffer (pH 9.0). After washing in phosphate-buffered saline, nonspecific antigens were blocked by incubation of the slides with 1% normal goat serum for 20 min. The sections were then incubated with 1:200 diluted anti-CCL2 antibody (Abcam, Tokyo, Japan) or 1:100 diluted anti-macrophage colony-stimulating factor (M-CSF) antibody (Abcam) at 4°C overnight. Tissue sections were treated with MAX-PO:R (Nichirei, Seattle, WA, USA) for 30 min and then incubated with simple stain DAB solution (Nichirei). Finally, sections were counterstained with hematoxylin, dehydrated, and mounted.

Hepa1-6 cell culture

The Hepa1-6 cell line, which is derived from a BW7756 tumor from a C57BL/6J mouse, was purchased from DS Pharma Biomedical Japan (Osaka, Japan). To observe the effect of steatosis in hepatocytes, Hepa1-6 cells were exposed to 0.1 mM oleic acid or palmitic acid (Wako Chemical, Osaka, Japan) for 3 h, as described previously [21]. Lipid accumulation was confirmed by Sudan III staining [21]. The concentrations of CCL2 present in culture supernatants were estimated by ELISAs.

Real-time reverse transcription polymerase chain reaction

RNA was extracted from livers and the Hepa 1–6 cell line using the RNeasy Plus Mini Kit (Qiagen, Hilden, Germany). Reverse transcription reactions were performed using the High-Capacity cDNA Reverse Transcription kit (Applied Biosystems, Foster City, CA, USA), and real-time polymerase chain reaction analysis was performed using SYBR Green I (Roche Diagnostics, Basel, Switzerland) on a LightCycler 480II (Roche Diagnostics). The pairs of sequence-specific primers that were used are listed in [S1 Table](#).

Induction of bone marrow-derived monocytic MDSCs by M-CSF

Bone marrow cells were obtained by flushing the tibias of C57BL/6J mice, followed by red blood cell lysis. Cells were suspended in complete RPMI 1640 media supplemented with 10% heat-inactivated fetal bovine serum, and cultured with or without recombinant M-CSF (R&D). After 3 days, $CD11b^+Gr1^{\text{dim}}Ly6C^{\text{high}}$ and $CD11b^+Gr1^{\text{dim}}Ly6C^{\text{low}}$ cells were sorted to allow testing of their functions in the allogenic mixed lymphocyte reaction assay.

Statistical analyses

Data were analyzed using JMP 8.0 software (SAS Institute, Cary, NC, USA). Values are presented as means \pm SEM. A Student's *t*-test was employed to compare data between 2 groups. For multiple comparisons, a one-way ANOVA was used. $P < 0.05$ was considered significant.

Results

Expansion of liver $SSC^{\text{low}}CD11b^+Gr1^{\text{dim}}$ cells by a high-fat diet

In NAFLD mice, the frequency of liver $CD11b^+Gr1^+$ cells was significantly increased compared with that in control mice, as previously reported [14, 15]. We found that the frequency of liver $CD11b^+Gr1^+$ cells increased in high-fat diet fed mice over time (Fig 1A). As previously reported [20], these cells could be grouped into 2 subtypes: $CD11b^+Gr1^{\text{dim}}$ and $CD11b^+Gr1^{\text{high}}$. Additional examination by SSC, a measure of cell granularity, revealed that the $Gr1^{\text{high}}$ subtype consisted of only 1 population; however, the $Gr1^{\text{dim}}$ subtype could be further divided into SSC^{high} and SSC^{low} populations (Fig 1B). The frequency of $SSC^{\text{high}}CD11b^+Gr1^{\text{dim}}$ cells was increased at 3 months of age in NAFLD mice compared to that in control mice; however, the frequency of these cells was decreased in mice fed with a high-fat diet at 12 months. In NAFLD mice, the frequency of the $SSC^{\text{low}}CD11b^+Gr1^{\text{dim}}$ cells was significantly higher than that in control mice, and the number of cells increased in the high-fat diet mice over time (Fig 1C).

Characteristics of $CD11b^+Gr1^+$ cell subsets

Liver $CD11b^+Gr1^+$ cells were further characterized by examining the expression of cell surface markers and morphology. These cells expressed CD45. $SSC^{\text{low}}CD11b^+Gr1^{\text{dim}}$ cells expressed $Ly6C^{\text{high}}$, whereas $SSC^{\text{high}}CD11b^+Gr1^{\text{dim}}$ and $CD11b^+Gr1^{\text{high}}$ cells expressed $Ly6C^{\text{low}}$. $Ly6G$ was detected only on $CD11b^+Gr1^{\text{high}}$ cells. CCR2, CD115, CD274, and CD80 were detected only on $SSC^{\text{low}}CD11b^+Gr1^{\text{dim}}$ cells, and CD31 was detected only on $SSC^{\text{high}}CD11b^+Gr1^{\text{dim}}$ cells. F4/80 was detected on both SSC^{high} and SSC^{low} $CD11b^+Gr1^{\text{dim}}$ cells; however, the expression level in the SSC^{high} population was higher than that in the SSC^{low} population. None of subsets expressed CD11c (Fig 2A). Wright-Giemsa staining demonstrated that $CD11b^+Gr1^{\text{high}}$ cells had lobular-shaped nuclei, typical of granulocytes, whereas $SSC^{\text{high}}CD11b^+Gr1^{\text{dim}}$ and $SSC^{\text{low}}CD11b^+Gr1^{\text{dim}}$ cells had ovoid nuclei, typical of monocytes/macrophages. Additionally, the SSC^{high} population was larger in size than the SSC^{low} population (SSC^{high} population: $6.81 \pm 0.31 \mu\text{m}$; SSC^{low} population: $5.17 \pm 0.25 \mu\text{m}$), as shown in Fig 2B ($n = 5$; $p < 0.05$).

Immunosuppressive function of $SSC^{\text{low}}CD11b^+Gr1^{\text{dim}}$ cells

We found that liver $SSC^{\text{low}}CD11b^+Gr1^{\text{dim}}$ cells suppressed T cell proliferation; however, $SSC^{\text{high}}CD11b^+Gr1^{\text{dim}}$ cells did not affect T cell proliferation (Fig 3A). In addition, the frequency of IFN- γ -producing T cells decreased after co-culturing with $SSC^{\text{low}}CD11b^+Gr1^{\text{dim}}$ cells (Fig 3B). Based on allogenic mixed lymphocyte reaction assays, liver $SSC^{\text{low}}CD11b^+Gr1^{\text{dim}}$ cells suppressed allogeneic T cell proliferation in a dose-dependent manner. The suppressive activity was remarkably effective, even at a ratio of 1:200. Similar to the results shown in Fig 3A, $SSC^{\text{high}}CD11b^+Gr1^{\text{dim}}$ cells exhibited no suppressive ability in the allogenic mixed lymphocyte reactions (Fig 3C).

$SSC^{\text{low}}CD11b^+Gr1^{\text{dim}}$ MDSCs inhibit T cell proliferation via a NO-dependent mechanism

iNOS, arginase 1, or ROS inhibitor was added to the co-culture. Neither nor-NOHA (an arginase 1 inhibitor) nor catalase (a ROS inhibitor) affected T cell proliferation. However, the

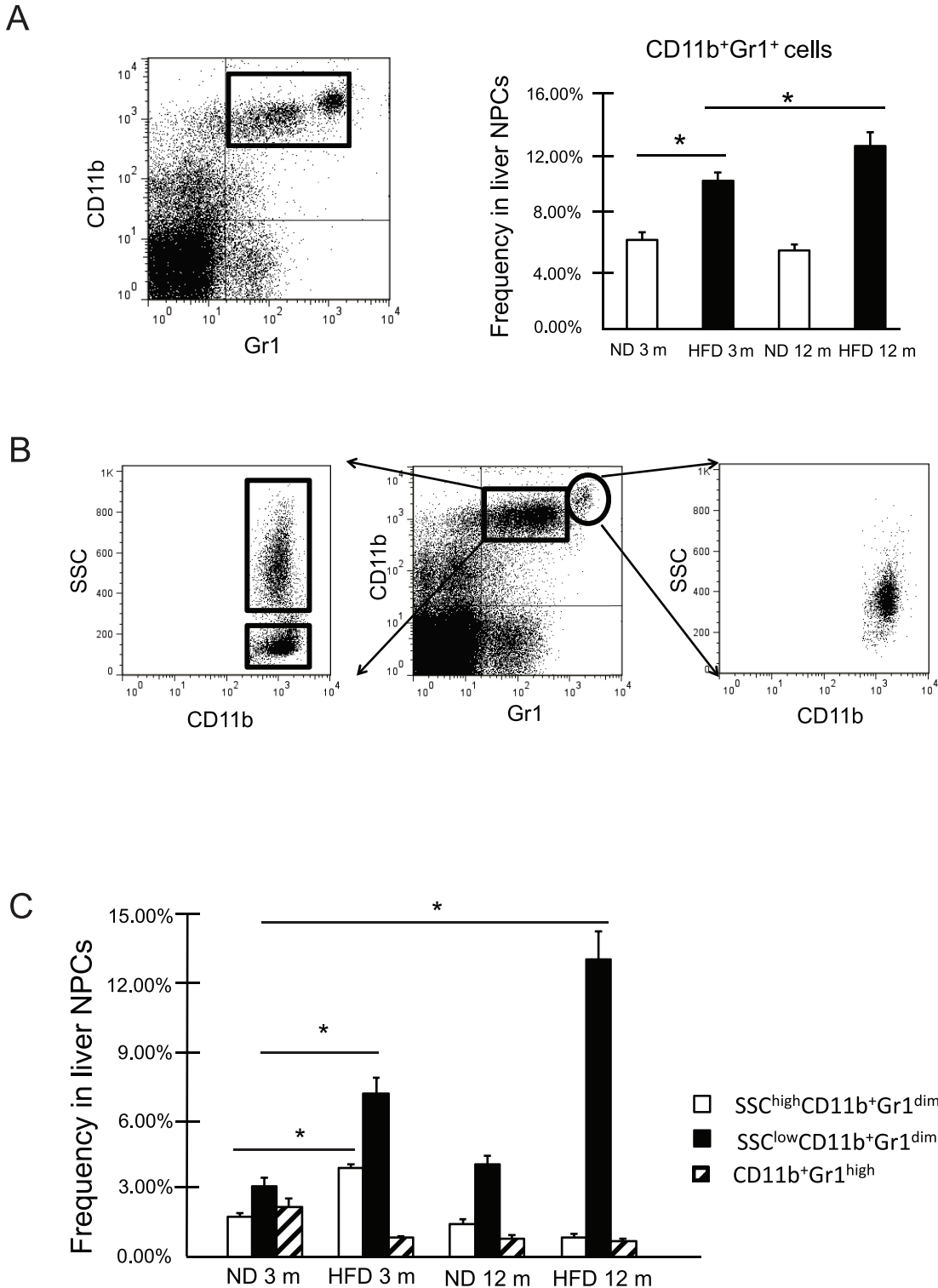
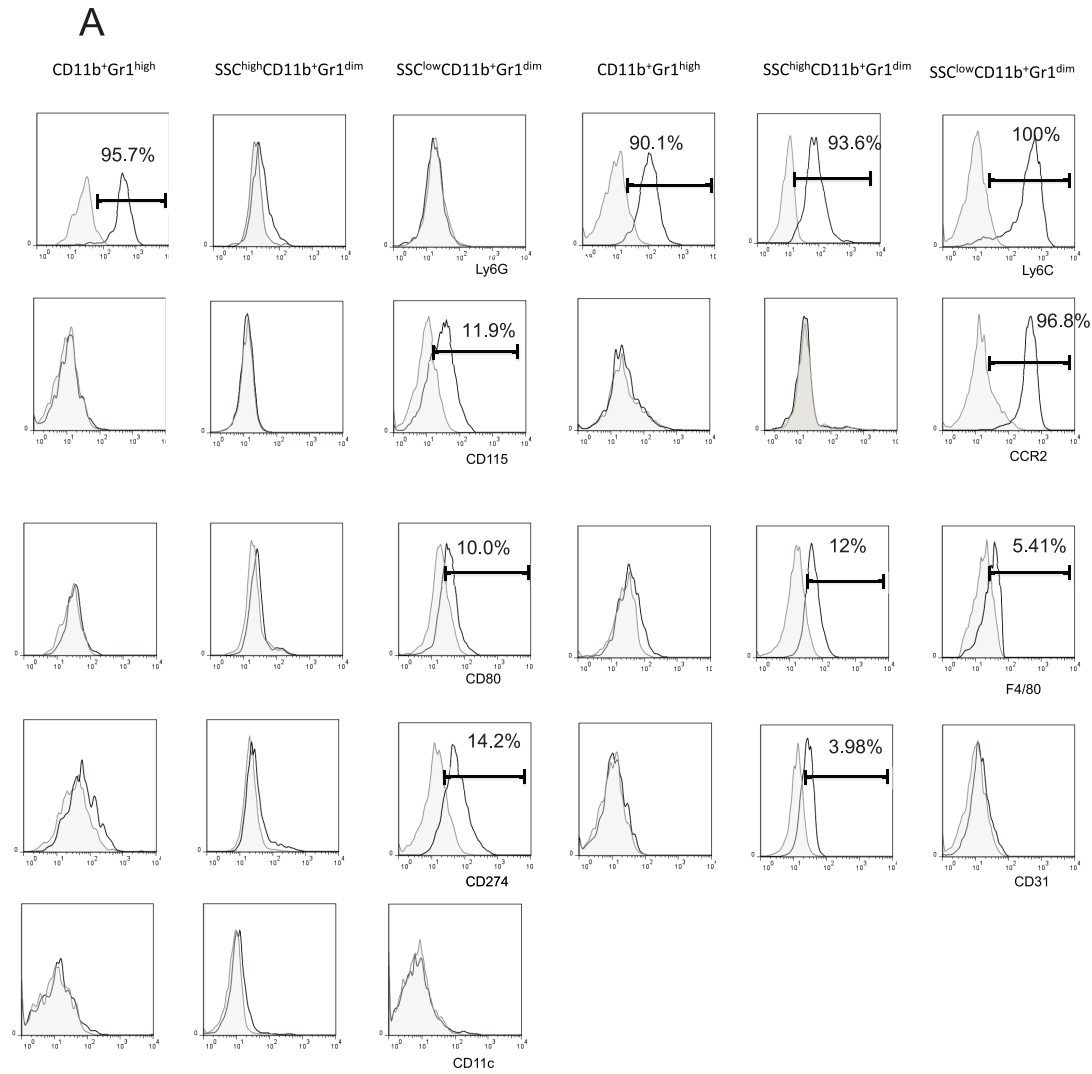


Fig 1. CD11b⁺Gr1⁺ cells in the livers of normal mice and high-fat-diet mice were comprised of 3 subsets. (A) Frequency of CD11b⁺Gr1⁺ cells in mouse liver non-parenchymal cells (NPCs) at 3 months (3 m) or 12 months (12 m) of age (n = 5). **P* < 0.05 (B) Analysis of CD11b⁺Gr1⁺ cells by the side-scatter (SSC) of light during flow cytometry. (C) Frequency of CD11b⁺Gr1^{high}, SSC^{low}CD11b⁺Gr1^{dim}, and SSC^{high}CD11b⁺Gr1^{dim} cells in mouse liver NPCs at 3 m or 12 m of age (n = 5). **P* < 0.05 compared to frequency of each cells at 3 months. ND, normal diet; HFD, high fat diet.

doi:10.1371/journal.pone.0149948.g001



B

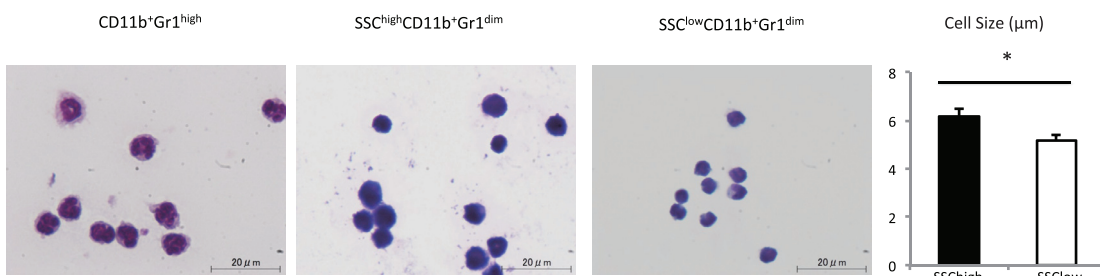


Fig 2. Characterization of liver CD11b⁺Gr1⁺ cell subsets. (A) Representative histograms of the phenotypic profiles of liver CD11b⁺Gr1^{high}, SSC^{high}CD11b⁺Gr1^{dim}, and SSC^{low}CD11b⁺Gr1^{dim} cells. Closed histograms represent background control staining; open histograms represent staining by indicated monoclonal antibody (mAb). The percentage of positive cells is indicated. (B) Morphology of purified liver CD11b⁺Gr1^{high}, SSC^{high}CD11b⁺Gr1^{dim}, and SSC^{low}CD11b⁺Gr1^{dim} cells by Wright-Giemsa staining (100× magnification). Scale bars, 20 µm. SSC, light side scatter. The sizes of SSC^{high}CD11b⁺Gr1^{dim} and SSC^{low}CD11b⁺Gr1^{dim} cells are shown in the right panel. **P* < 0.05

doi:10.1371/journal.pone.0149948.g002

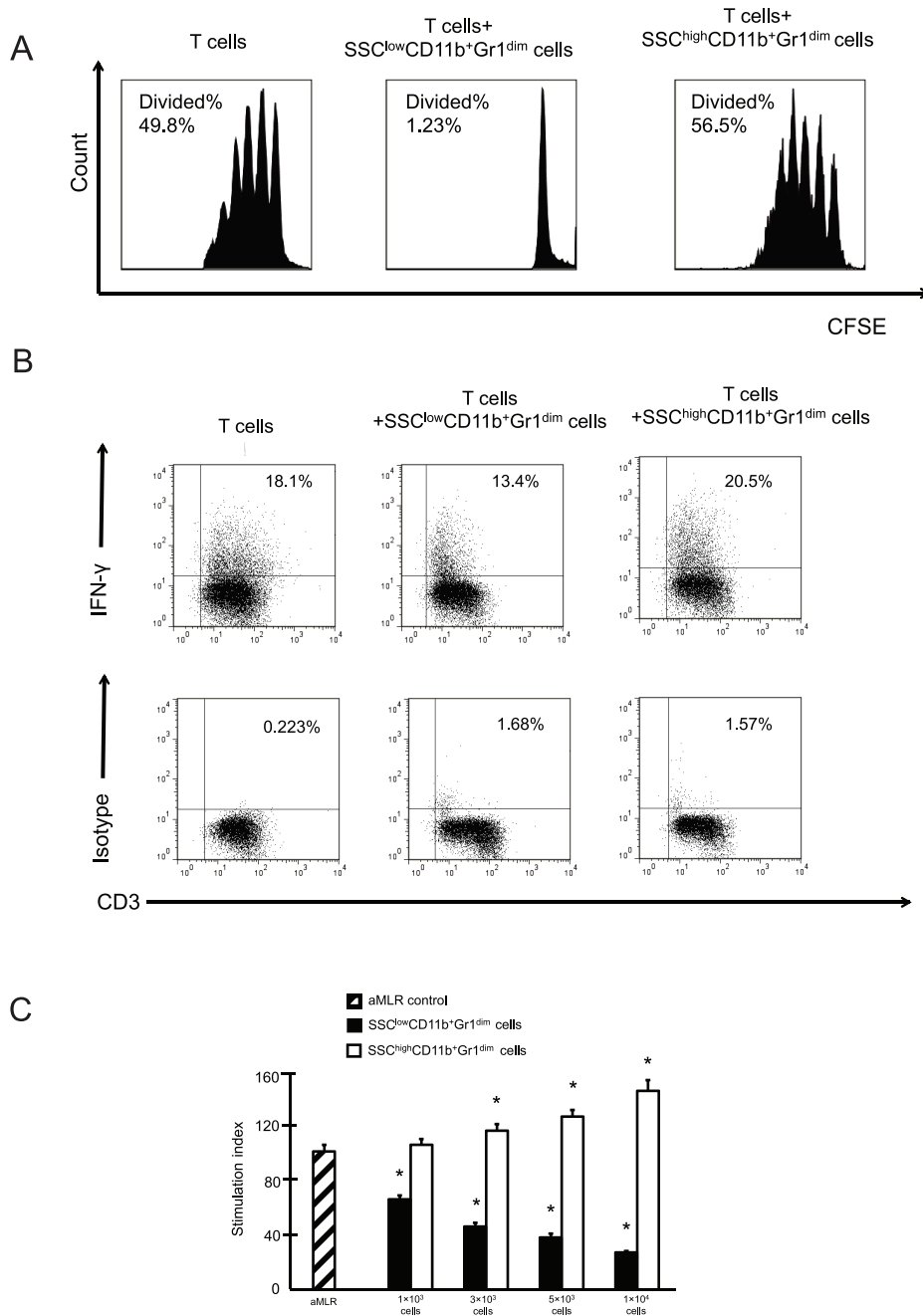


Fig 3. SSC^{low}CD11b⁺Gr1^{dim} cells in the livers suppress T cell responses. (A) Proliferation of CFSE-labeled T cells cultured in the presence of Dynabeads mouse T-Activator CD3/CD28 with or without liver SSC^{high} or SSC^{low} CD11b⁺Gr1^{dim} cells. (B) Representative image of intracellular interferon-γ staining for T cells cultured with or without liver SSC^{high} or SSC^{low} CD11b⁺Gr1^{dim} cells. (C) T cells and allogenic dendritic cells were co-cultured. Liver SSC^{high} and SSC^{low}CD11b⁺Gr1^{dim} cells were added to the cultures. The data obtained from 3 separate experiments are shown. **P* < 0.05 compared to the levels of T cell proliferation in allogenic mixed lymphocyte reactions (aMLRs) without CD11b⁺Gr1^{dim} cells.

doi:10.1371/journal.pone.0149948.g003

addition of L-NIL, an iNOS inhibitor, restored T cell proliferation (Fig 4A). The level of nitrite in the supernatants of T cells or liver $SSC^{\text{low}}CD11b^+Gr1^{\text{dim}}$ MDSCs alone was below the threshold of detection. However, after T cells and liver $SSC^{\text{low}}CD11b^+Gr1^{\text{dim}}$ MDSCs were co-cultured, nitrite was produced in the supernatants at detectable levels (Fig 4B). Liver $SSC^{\text{low}}CD11b^+Gr1^{\text{dim}}$ MDSCs cultured alone did not express iNOS, whereas after they were co-cultured with T cells, iNOS expression was detected. The T cells had no independent ability to express iNOS (Fig 4C). These results indicated that the role of liver $SSC^{\text{low}}CD11b^+Gr1^{\text{dim}}$ cells is distinct from that of their cognate $SSC^{\text{high}}CD11b^+Gr1^{\text{dim}}$ cells, representing an authentic phenotype of monocytic MDSCs in the liver.

$SSC^{\text{low}}CD11b^+Gr1^{\text{dim}}$ MDSCs might be recruited to the NAFLD liver via the CCL2-CCR2 pathway

Chemokines recruit immune cells to inflamed sites. As shown in Fig 2, $SSC^{\text{low}}CD11b^+Gr1^{\text{dim}}$ MDSCs expressed the receptor for the chemokine CCL2, CCR2. We found that the *CCL2* mRNA expression level was increased in the livers of NAFLD mice (Fig 5A), as was CCL2 protein expression (Fig 5B and 5C). Although hepatocytes treated with normal diet for 12 months showed some changes in fat contents, this finding may have been related to age-induced triglyceride accumulation [22]. As some studies have generated hepatocyte steatosis models by culturing cells with fatty acids (oleic and palmitic acid) *in vitro* [23, 24], we confirmed these results using Hepa1-6 cells supplemented with 0.1 mM oleic acid or palmitic acid. *CCL2* mRNA expression increased with lipid accumulation *in vitro* (Fig 5D). In addition, CCL2 protein secretion from Hepa 1–6 cells (558.2 ± 22.8 pg/ml) increased compared with that from cells treated with oleic acid (605.2 ± 13.1 pg/ml) or palmitic acid (590.4 ± 8.7 pg/ml) ($n = 5$; $p < 0.05$). These data suggest that steatosis induces increased CCL2 expression in hepatocytes. Finally, we evaluated the migratory capacity of $SSC^{\text{low}}CD11b^+Gr1^{\text{dim}}$ MDSCs, and found that these cells migrated in response to CCL2 in a dose-dependent manner (Fig 5F).

Induction of $SSC^{\text{low}}CD11b^+Gr1^{\text{dim}}$ MDSCs in the NAFLD liver might be associated with M-CSF upregulation

$SSC^{\text{low}}CD11b^+Gr1^{\text{dim}}$ MDSCs expressed the M-CSF receptor CD115. M-CSF has previously been shown to play an important role in the development and induction of MDSCs [7]. We found that the mRNA expression of *M-CSF* was higher in the livers of NAFLD mice than control mice (Fig 6A). The protein expression of M-CSF was also increased in hepatocytes, as well as in non-parenchymal cells of NAFLD mouse livers (Fig 6B). The increased expression of M-CSF was confirmed using Hepa1-6 cells cultured with fatty acid (oleic or palmitic acid) (Fig 6C), indicating that steatotic hepatocytes produce M-CSF. To confirm the role of M-CSF in the induction of MDSCs, we cultured bone marrow cells with or without recombinant M-CSF for 3 days. $CD11b^+Gr1^{\text{dim}}$ cells in the bone marrow were divided into 2 subtypes, which showed low ($Ly6C^{\text{low}}$) or high ($Ly6C^{\text{high}}$) *Ly6C* expression. $CD11b^+Gr1^{\text{dim}}Ly6C^{\text{high}}$ cells in the bone marrow are phenotypically similar to $SSC^{\text{low}}CD11b^+Gr1^{\text{dim}}$ MDSCs in the liver (S1 Fig). These cells showed an increased prevalence in cultures grown in the presence of M-CSF in a dose-dependent manner (Fig 6D). In addition, $CD11b^+Gr1^{\text{dim}}Ly6C^{\text{high}}$ these cells, but not other $CD11b^+Gr1^{\text{dim}}$ cells in the bone marrow, exhibited immunosuppressive ability (Fig 6E).

Discussion

The liver is a primary site for MDSC induction and accumulation. Recently, several studies have linked these cells to the pathogenesis of HCC, hepatitis, or liver fibrosis [9,10,12]. In this

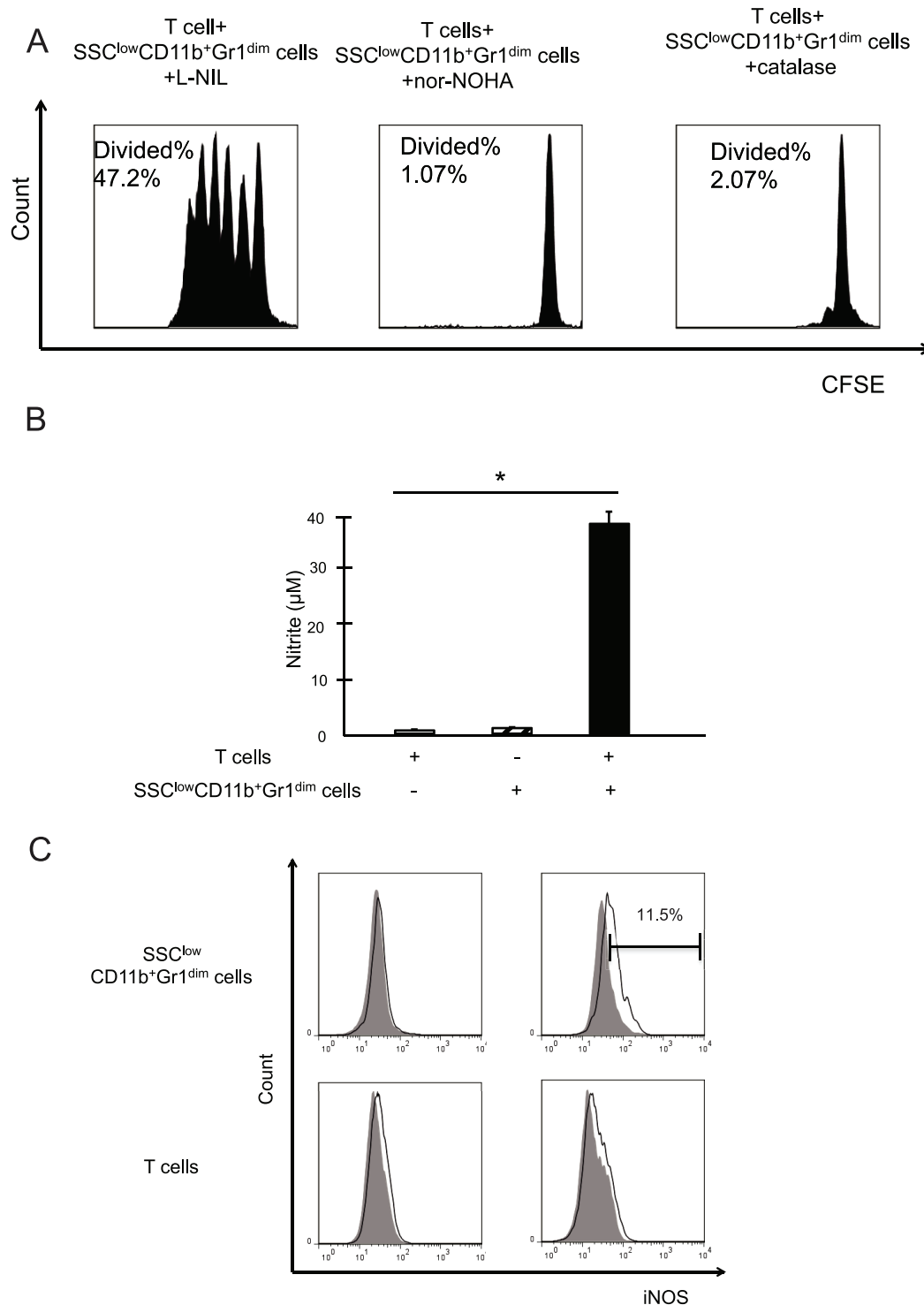


Fig 4. The suppressive function of liver SSC^{low}CD11b⁺Gr1^{dim} cells is dependent on a NO mechanism. (A) Proliferation of carboxy-fluorescein diacetate, succinimidyl ester (CFSE)-labeled T cells cultured in the presence of Dynabeads mouse T-Activator CD3/CD28 along with purified liver SSC^{low}CD11b⁺Gr1^{dim} cells. Different enzyme inhibitors (L-NIL, nor-NOHA, or catalase) were added at the start of each respective culture. (B) Nitrite levels were investigated in the culture supernatants after 60 h of co-culture (n = 3). (C) The intracellular iNOS expression was determined by flow cytometry. The percentage of positive cells is indicated. The data obtained from 3 separate experiments are shown. *P < 0.05 compared to T cells alone.

doi:10.1371/journal.pone.0149948.g004

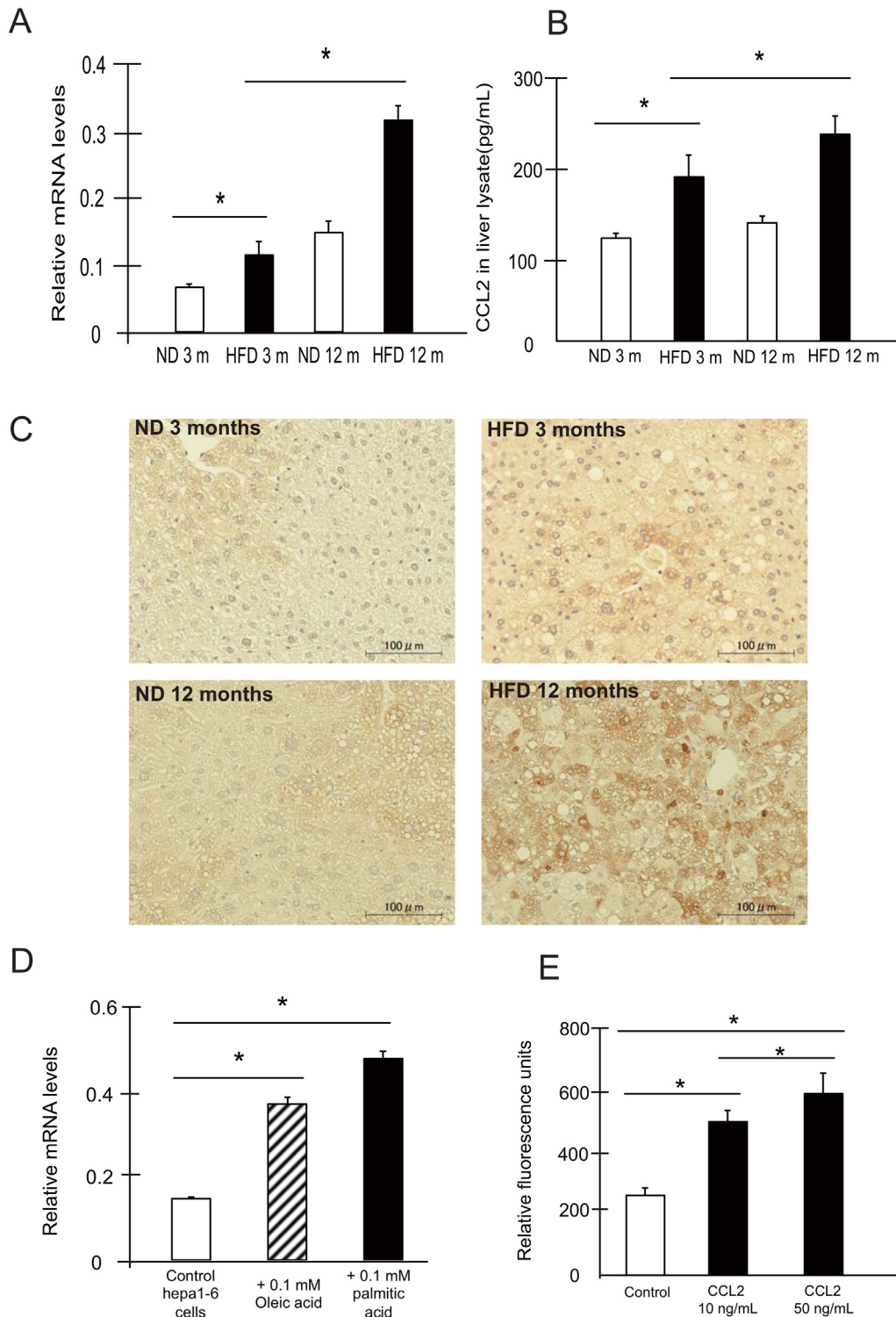


Fig 5. The CCL2/CCR2 pathway mediates the migration of $SSC^{low}CD11b^{+}Gr1^{dim}$ cells to the NAFLD liver. (A) *CCL2* expression in the livers of ND and HFD-fed mice was investigated by real-time RT-PCR (n = 5). (B, C) Protein expression of CCL2 in the livers was investigated by ELISA (B) (n = 5) and immunohistochemistry (C). Scale bars, 100 μ m. (D) *CCL2* gene expression in Hepa1-6 cells treated with oleic acid or palmitic acid analyzed by real-time RT-PCR (n = 5). (E) Migration assays revealed that $SSC^{low}CD11b^{+}Gr1^{dim}$ cells migrated in response to CCL2 *in vitro* (n = 5). **P* < 0.05

doi:10.1371/journal.pone.0149948.g005

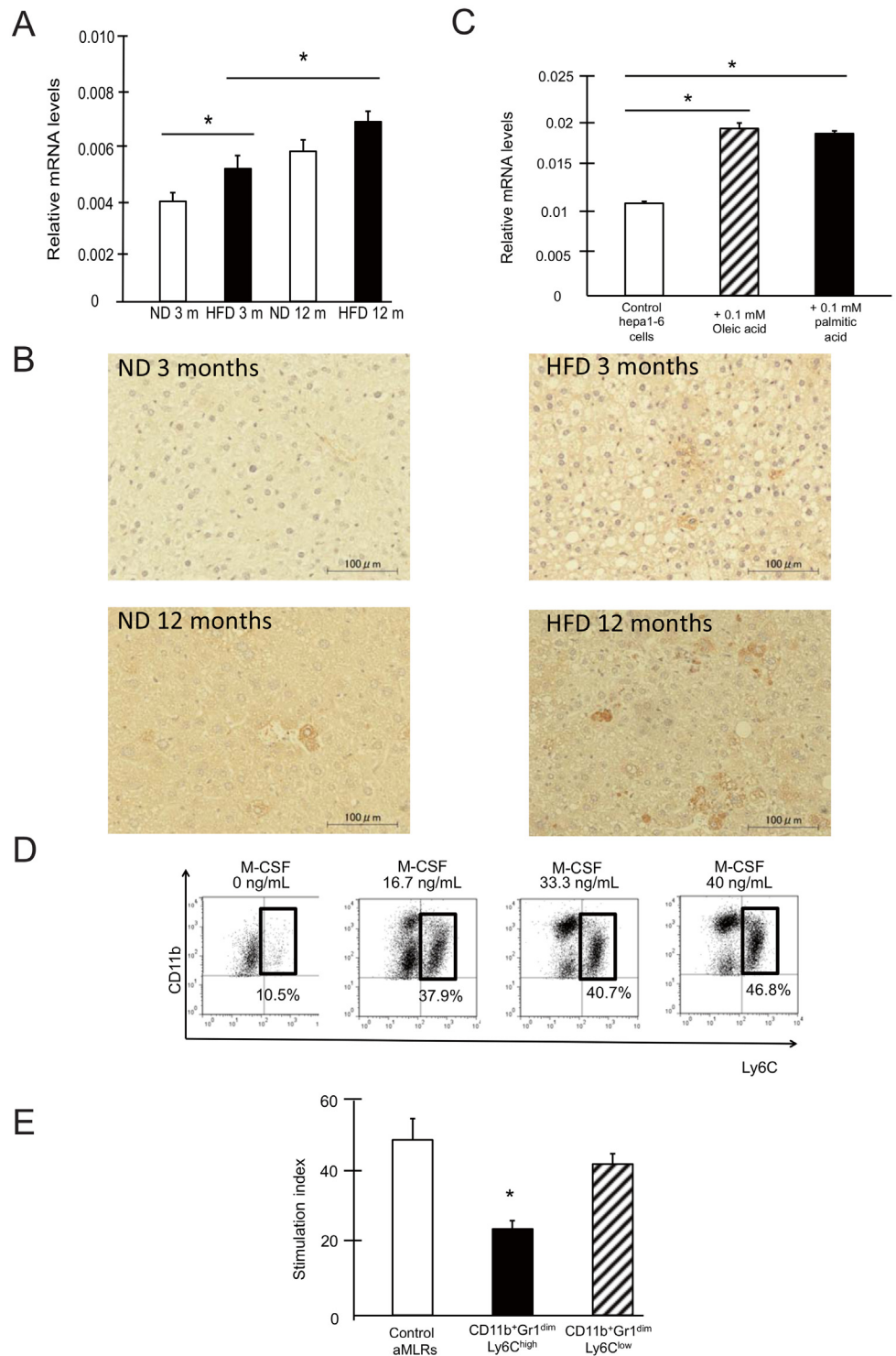


Fig 6. M-CSF is associated with SSC^{low}CD11b⁺Gr1^{dim} cell expansion in the liver. (A) Liver M-CSF mRNA was investigated by real-time RT-PCR (n = 5). (B) Liver M-CSF protein was investigated by immunohistochemistry (n = 5). Scale bars, 100 μm. (C) M-CSF mRNA in Hepa1-6 cells treated with fatty acid was analyzed by real-time RT-PCR (n = 5). (D) Bone marrow cells were cultured with M-CSF. The frequency of CD11b⁺Gr1^{dim}Ly6C^{high} cells among the CD11b⁺Gr1^{dim} cells is shown. (E) The Ly6C^{high} and Ly6C^{low} populations (S1 Fig) were sorted and added to allogenic MLRs. *P < 0.05

doi:10.1371/journal.pone.0149948.g006

study, we found that liver CD11b⁺Gr1^{dim} cells, which are monocytic MDSCs in general, could be divided into 2 phenotypes, SSC^{high} and SSC^{low} populations. SSC^{low}CD11b⁺Gr1^{dim} cells accumulated in the livers of NAFLD mice (Fig 1). These enlarged SSC^{low} populations had a strong suppressive effect against T cells (Fig 3) and expressed Ly6C^{high}, CCR2, CD115, CD80, and CD274 (Fig 2A), which are characteristic of MDSCs in tumors [16, 25]. Morphologic assessment showed that these were monocyte-derived cells (Fig 2B). In contrast, the SSC^{high} populations expressed Ly6C^{low}, F4/80, and CD31 (Fig 2A). Although CD31 was found to be a marker of MDSCs in some previous studies [20, 26], the SSC^{high} populations activated T cell proliferation (Fig 3). CD11b⁺Gr1^{high} cells expressed Ly6G^{high} and Ly6C^{low} antigens and had a granulocytic morphology (Fig 2). Because this population was present at a very low level in the livers of NAFLD mice, we did not investigate their function in T cell proliferation. However, some studies have shown that these granulocytic CD11b⁺Gr1^{high} cells from mouse livers also exert a suppressive effect on T cells, but that this suppressive activity is weaker than that of CD11b⁺Gr1^{dim} cells [20, 27].

Obesity is a chronic low-grade inflammatory condition. Lymphocytes are often detected in the lobular infiltrates of obese livers [28], and it is believed that these cells contribute to the progression of NAFLD, which is associated with an increased production of cytokines and exacerbated liver parenchymal injury and fibrosis [4]. The depletion of liver MDSCs has been shown to enhance fibrosis markers [12], suggesting a protective role for MDSCs in liver fibrosis. Other studies have demonstrated that MDSCs exhibit protective and immunosuppressive properties during host infection [11, 29]. Concordantly, the results of this study revealed that liver SSC^{low}CD11b⁺Gr1^{dim} MDSCs have a strong suppressive effect on T cells (Fig 3). The accumulation of SSC^{low}CD11b⁺Gr1^{dim} MDSCs in livers of NAFLD might allow them to function as critical “homeostatic” regulators to counteract proinflammatory cells. Depletion of SSC^{low} MDSCs may provide important information regarding their contribution to NAFLD. However, antibodies or pharmacological inhibitors to specifically target these cells have not been established, as of yet. Future studies regarding this point need to be conducted.

At the mechanistic level, the suppressive activity of MDSCs has been associated with L-arginine metabolism. L-Arginine is a substrate for iNOS, which is highly expressed in MDSCs [7]. NO production via this pathway is a powerful modulator of inflammation and has been reported to preferentially inhibit T cell immune responses [30, 31]. NO suppresses T cell function by blocking the activation of several important signaling molecules in T cells [32]. NO has also been shown to suppress MHC class II expression and promote T cell apoptosis [33, 34]. Our study demonstrated that liver SSC^{low}CD11b⁺Gr1^{dim} MDSC inhibition of T cell proliferation is dependent on NO production by iNOS (Fig 4), consistent with these studies. However, further research is necessary to clarify the mechanisms of iNOS induction in MDSCs that occurs after co-culture with T cells.

The results of several studies provide a link between chemokines and MDSC accumulation in the liver in HCC [35, 36]. The CCL2/CCR2 chemokine axis plays a pivotal role in the migration of MDSCs in cancer, and impairment of CCL2/CCR2 signaling inhibits tumor growth [37–39]. In this study, we found that the expression of CCL2 was up-regulated in the livers of NAFLD mice, and that CCL2 could stimulate the migration of SSC^{low}CD11b⁺Gr1^{dim} MDSCs *in vitro* (Fig 5). Thus, the CCL2-CCR2 pathway might contribute to SSC^{low}CD11b⁺Gr1^{dim} MDSC accumulation in the steatotic liver.

M-CSF regulates the proliferation, differentiation, chemotaxis, and survival of mononuclear phagocytic cells through its action on CD115 [40]. Recent studies have shown that M-CSF expression is correlated with the expansion of MDSCs [7], and that blocking CD115 inhibits the immunosuppressive tumor milieu and facilitates immune responses, resulting in improved antitumor T-cell function [41]. In this study, we found that M-CSF expression was higher in

the livers of NAFLD mice than control mice. In addition, M-CSF induced the expansion of monocytic MDSCs *in vitro* (Fig 6). These results suggest that the increased level of M-CSF in the steatotic liver might contribute to the increase in the frequency of SSC^{low}CD11b⁺Gr1^{dim} MDSCs.

Previous data have shown that MDSCs accumulate in mouse models of HCC and may play critical roles in the immune escape of tumor cells [7]. Obesity and NAFLD are recognized as major risk factors of HCC [42]. Although further studies are necessary, it appears likely that the increased frequency of MDSCs in NAFLD contributes to HCC pathogenesis. Recently, an increased frequency of MDSCs in NAFLD patients was reported [43]. Additional clinical research regarding the role of MDSCs in HCC and NAFLD should be pursued.

In conclusion, we identified SSC^{low}CD11b⁺Gr1^{dim} as the authentic phenotype of liver monocytic MDSCs and showed that these exhibit a strong suppressive effect on T cells. In addition, these cells inhibited T cells via NO production by iNOS. Our results suggest that the accumulation of MDSCs in the liver might regulate the immune environment of NAFLD.

Supporting Information

S1 Fig. Subtypes of CD11b⁺Gr1^{dim} cells in the bone marrow and liver NPCs. (A) Subtypes of CD11b⁺Gr1^{dim} cells in the bone marrow after culturing in the presence of M-CSF. (B) Subtypes of CD11b⁺Gr1^{dim} cells in liver NPCs. (EPS)

S1 Table. Primer sequences for real-time reverse transcription-polymerase chain reaction amplification. (DOCX)

Acknowledgments

We thank Ms. Sakiko Sugawara, Ms. Ayumi Sumisaki, and Mr. Kenji Tanimoto for their valuable contributions to this study.

Author Contributions

Conceived and designed the experiments: LY MA MO YH. Performed the experiments: LY MA KK. Analyzed the data: LY MA KK. Contributed reagents/materials/analysis tools: MA KK. Wrote the paper: LY MA SMFA BM MO YH.

References

1. Chalasani N, Younossi Z, Lavine JE, Diehl AM, Brunt EM, Cusi K, et al. The diagnosis and management of non-alcoholic fatty liver disease: practice guidelines by the American Gastroenterological Association, American Association for the study of Liver diseases, and American College of Gastroenterology. *Gastroenterology*. 2012; 142: 1592–1609. doi: [10.1053/j.gastro.2012.04.001](https://doi.org/10.1053/j.gastro.2012.04.001) PMID: [22656328](https://pubmed.ncbi.nlm.nih.gov/22656328/)
2. Michelotti GA, Machado MV, Diehl AM. NAFLD, NASH and liver cancer. *Nat Rev Gastroenterol Hepatol*. 2013; 10: 656–665. doi: [10.1038/nrgastro.2013.183](https://doi.org/10.1038/nrgastro.2013.183) PMID: [24080776](https://pubmed.ncbi.nlm.nih.gov/24080776/)
3. Tilg H, Mochen AR. Evolution of inflammation in non-alcoholic fatty liver disease: the multiple parallel hypothesis. *Hepatology*. 2010; 52: 1836–1846. doi: [10.1002/hep.24001](https://doi.org/10.1002/hep.24001) PMID: [21038418](https://pubmed.ncbi.nlm.nih.gov/21038418/)
4. Sutti S, Jindal A, Locatelli I, Vacchiano M, Gigliotti L, Bozzola C, et al. Adaptive immune responses triggered by oxidative stress contribute to hepatic inflammation in NASH. *Hepatology*. 2014; 59: 886–897. doi: [10.1002/hep.26749](https://doi.org/10.1002/hep.26749) PMID: [24115128](https://pubmed.ncbi.nlm.nih.gov/24115128/)
5. Ma X, Hua J, Mohamood AR, Hamad AR, Ravi R, Li Z. A high-fat diet and regulatory T cells influence susceptibility to endotoxin-induced liver injury. *Hepatology* 2007; 46: 1519–1529. PMID: [17661402](https://pubmed.ncbi.nlm.nih.gov/17661402/)

6. Wan J, Benkdane M, Teixeira-Clerc F, Bonnafous S, Louvet A, Lafdil F, et al. M2 Kupffer cells promote M1 Kupffer cell apoptosis: a protective mechanism against alcoholic and nonalcoholic fatty liver disease. *Hepatology*. 2014; 59: 130–142. doi: [10.1002/hep.26607](https://doi.org/10.1002/hep.26607) PMID: [23832548](https://pubmed.ncbi.nlm.nih.gov/23832548/)
7. Gabrilovich DI, Nagaraj S. Myeloid-derived suppressor cells as regulators of the immune system. *Nat Rev Immunol*. 2009; 9: 162–174. doi: [10.1038/nri2506](https://doi.org/10.1038/nri2506) PMID: [19197294](https://pubmed.ncbi.nlm.nih.gov/19197294/)
8. Gabrilovich DI, Ostrand-Rosenberg S, Bronte V. Coordinated regulation of myeloid cells by tumours. *Nat Rev Immunol*. 2012; 4: 253–268.
9. Shen P, Wang A, He M, Wang Q, Zheng S. Increased circulating Lin^{low}CD33⁺HLA-DR⁻ myeloid-derived suppressor cells in hepatocellular carcinoma patients. *Hepatol Res*. 2014; 44: 639–650. doi: [10.1111/hepr.12167](https://doi.org/10.1111/hepr.12167) PMID: [23701406](https://pubmed.ncbi.nlm.nih.gov/23701406/)
10. Zeng QL, Yang B, Sun HQ, Feng GH, Jin L, Zou ZS, et al. Myeloid-derived suppressor cells are associated with viral persistence and downregulation of TCR zeta chain expression on CD8⁺ T cells in chronic hepatitis C patients. *Mol Cells*. 2014; 37: 66–73. doi: [10.14348/molcells.2014.2282](https://doi.org/10.14348/molcells.2014.2282) PMID: [24552712](https://pubmed.ncbi.nlm.nih.gov/24552712/)
11. Cripps JG, Wang J, Maria A, Blumenthal I, Gorham JD. Type 1 T helper cells induce the accumulation of myeloid-derived suppressor cells in the inflamed Tgfb1 knockout mouse liver. *Hepatology*. 2010; 52: 1350–1359. doi: [10.1002/hep.23841](https://doi.org/10.1002/hep.23841) PMID: [20803559](https://pubmed.ncbi.nlm.nih.gov/20803559/)
12. Höchst B, Mikulec J, Baccega T, Metzger C, Welz M, Peusquens J, et al. Differential induction of Ly6G and Ly6C positive myeloid derived suppressor cells in chronic kidney and liver inflammation and fibrosis. *PLoS One*. 2015; 10: e0119662. doi: [10.1371/journal.pone.0119662](https://doi.org/10.1371/journal.pone.0119662) PMID: [25738302](https://pubmed.ncbi.nlm.nih.gov/25738302/)
13. Kong X, Sun R, Chen Y, Wei H, Tian Z. $\gamma\delta$ T cells drive myeloid-derived suppressor cell-mediated CD8⁺ T cell exhaustion in Hepatitis B virus-induced immunotolerance. *J Immunol*. 2014; 193: 1645–1653. doi: [10.4049/jimmunol.1303432](https://doi.org/10.4049/jimmunol.1303432) PMID: [25015833](https://pubmed.ncbi.nlm.nih.gov/25015833/)
14. Xia S, Sha H, Yang L, Ji Y, Ostrand-Rosenberg S, Qi L. Gr-1⁺CD11b⁺myeloid-derived suppressor cells suppress inflammation and promote insulin sensitivity in obesity. *J Biol Chem*. 2011; 286: 23591–23599. doi: [10.1074/jbc.M111.237123](https://doi.org/10.1074/jbc.M111.237123) PMID: [21592961](https://pubmed.ncbi.nlm.nih.gov/21592961/)
15. Chen S, Akbar SM, Miyake T, Abe M, Al-Mahtab M, Furukawa S, et al. Diminished immune response to vaccinations in obesity: role of myeloid-derived suppressor and other myeloid cells. *Obes Res Clin Pract*. 2015; 9: 35–44. doi: [10.1016/j.orcp.2013.12.006](https://doi.org/10.1016/j.orcp.2013.12.006) PMID: [25660173](https://pubmed.ncbi.nlm.nih.gov/25660173/)
16. Youn JI, Nagaraj S, Collazo M, Gabrilovich DI. Subsets of myeloid-derived suppressor cells in tumor bearing mice. *J Immunol*. 2008; 181: 5791–5802. PMID: [18832739](https://pubmed.ncbi.nlm.nih.gov/18832739/)
17. Blériot C, Dupuis T, Jouvion G, Eberl G, Disson O, and Lecuit M. Liver-resident macrophage necrosis orchestrates type 1 microbicidal inflammation and type-2-mediated tissue repair during bacterial infection. *Immunity*. 2015; 42: 145–158. doi: [10.1016/j.immuni.2014.12.020](https://doi.org/10.1016/j.immuni.2014.12.020) PMID: [25577440](https://pubmed.ncbi.nlm.nih.gov/25577440/)
18. Karlmark KR, Weiskirchen R, Zimmermann HW, Gassler N, Ginhoux F, Weber C, et al. Hepatic recruitment of the inflammatory Gr1⁺ monocyte subset upon liver injury promotes hepatic fibrosis. *Hepatology*. 2009; 50: 261–274. doi: [10.1002/hep.22950](https://doi.org/10.1002/hep.22950) PMID: [19554540](https://pubmed.ncbi.nlm.nih.gov/19554540/)
19. Deng ZB, Liu Y, Liu C, Xiang X, Wang J, Cheng Z, et al. Immature myeloid cells induced by a high-fat diet contribute to liver inflammation. *Hepatology*. 2009; 50: 1412–1420. doi: [10.1002/hep.23148](https://doi.org/10.1002/hep.23148) PMID: [19708080](https://pubmed.ncbi.nlm.nih.gov/19708080/)
20. Chen S, Akbar SM, Abe M, Hiasa Y, Onji M. Immunosuppressive functions of hepatic myeloid-derived suppressor cells of normal mice and in a murine model of chronic hepatitis B virus. *Clin Exp Immunol*. 2011; 166: 134–142. doi: [10.1111/j.1365-2249.2011.04445.x](https://doi.org/10.1111/j.1365-2249.2011.04445.x) PMID: [21762128](https://pubmed.ncbi.nlm.nih.gov/21762128/)
21. Kawasaki K, Abe M, Tada F, Tokumoto Y, Chen S, Miyake T, et al. Blockade of B-cell-activating factor signaling enhances hepatic steatosis induced by a high-fat diet and improves insulin sensitivity. *Lab Invest*. 2013; 93: 311–321. doi: [10.1038/abinvest.2012.176](https://doi.org/10.1038/abinvest.2012.176) PMID: [23318884](https://pubmed.ncbi.nlm.nih.gov/23318884/)
22. Xiong X, Wang X, Lu Y, Wang E, Zhang Z, Yang J, et al. Hepatic steatosis exacerbated by endoplasmic reticulum stress-mediated downregulation of FXR in aging mice. *J Hepatol*. 2014; 60: 847–854. doi: [10.1016/j.jhep.2013.12.003](https://doi.org/10.1016/j.jhep.2013.12.003) PMID: [24333182](https://pubmed.ncbi.nlm.nih.gov/24333182/)
23. Feldstein AE, Canbay A, Guicciardi ME, Higuchi H, Bronk SF, Gores GJ. Diet associated hepatic steatosis sensitizes to Fas mediated liver injury in mice. *J Hepatol*. 2003; 39: 978–983. PMID: [14642615](https://pubmed.ncbi.nlm.nih.gov/14642615/)
24. Tang Y, Bian Z, Zhao L, Liu Y, Liang S, Wang Q, et al. Interleukin-17 exacerbates hepatic steatosis and inflammation in non-alcoholic fatty liver disease. *Clin Exp Immunol*. 2011; 166: 281–290. doi: [10.1111/j.1365-2249.2011.04471.x](https://doi.org/10.1111/j.1365-2249.2011.04471.x) PMID: [21985374](https://pubmed.ncbi.nlm.nih.gov/21985374/)
25. Movahedi K, Guillemins M, Van den Bossche J, Van den Bergh R, Gysemans C, Beschin A, et al. Identification of discrete tumor-induced myeloid-derived suppressor cell subpopulations with distinct T cell-suppressive activity. *Blood*. 2008; 111: 4233–4244. doi: [10.1182/blood-2007-07-099226](https://doi.org/10.1182/blood-2007-07-099226) PMID: [18272812](https://pubmed.ncbi.nlm.nih.gov/18272812/)
26. Bronte V, Apolloni E, Cabrelle A, Ronca R, Serafini P, Zamboni P, et al. Identification of a CD11b(+)/Gr-1(+)/CD31(+) myeloid progenitor capable of activating or suppressing CD8(+) T cells. *Blood*. 2000; 96: 3838–3846. PMID: [11090068](https://pubmed.ncbi.nlm.nih.gov/11090068/)

27. Hegde VL, Dingh UP, Nagarkatti PS, and Nagarkatti M. Critical role of mast cells and peroxisome proliferator-activated receptor γ in the induction of myeloid-derived suppressor cells by marijuana cannabidiol in vivo. *J Immunol.* 2015; 194: 5211–5222. doi: [10.4049/jimmunol.1401844](https://doi.org/10.4049/jimmunol.1401844) PMID: [25917103](https://pubmed.ncbi.nlm.nih.gov/25917103/)
28. Brunt EM. Pathology of non-alcoholic fatty liver disease. *Nat Rev Gastroenterol Hepatol.* 2010; 7: 195–203. doi: [10.1038/nrgastro.2010.21](https://doi.org/10.1038/nrgastro.2010.21) PMID: [20195271](https://pubmed.ncbi.nlm.nih.gov/20195271/)
29. Tam JW, Kullas AL, Mena P, Bliska JB, van der Velden AW. CD11b+ Ly6Chi Ly6G- immature myeloid cells recruited in response to *Salmonella enterica serovar Typhimurium* infection exhibit protective and immunosuppressive properties. *Infect Immun.* 2014; 82: 2606–2614. doi: [10.1128/IAI.01590-13](https://doi.org/10.1128/IAI.01590-13) PMID: [24711563](https://pubmed.ncbi.nlm.nih.gov/24711563/)
30. Sosroseno W, Bird PS, Seymour GJ. Effect of exogenous nitric oxide on murine splenic immune response induced by *Aggregatibacter actinomycetemcomitans* lipopolysaccharide. *Anaerobe.* 2009; 15: 95–98. doi: [10.1016/j.anaerobe.2009.01.002](https://doi.org/10.1016/j.anaerobe.2009.01.002) PMID: [19402196](https://pubmed.ncbi.nlm.nih.gov/19402196/)
31. Sato K, Ozaki K, Oh I, Meguro A, Hatanaka K, Nagai T, et al. Nitric oxide plays a critical role in suppression of T-cell proliferation by mesenchymal stem cells. *Blood.* 2007; 109: 228–234. PMID: [16985180](https://pubmed.ncbi.nlm.nih.gov/16985180/)
32. Mazzoni A, Bronte V, Visintin A, Spitzer JH, Apolloni E, Serafini P, et al. Myeloid suppressor lines inhibit T cell responses by an NO-dependent mechanism. *J Immunol.* 2002; 168: 689–695. PMID: [11777962](https://pubmed.ncbi.nlm.nih.gov/11777962/)
33. Harari O, Liao JK. Inhibition of MHC II gene transcription by nitric oxide and antioxidants. *Curr Pharm Des.* 2004; 10: 893–898. PMID: [15032692](https://pubmed.ncbi.nlm.nih.gov/15032692/)
34. Rivoltini L, Carrabba M, Huber V, Castelli C, Novellino L, Dalerba P, et al. Immunity to cancer: attack and escape in T lymphocyte tumor cell interaction. *Immunol Rev.* 2002; 188: 97–113. PMID: [12445284](https://pubmed.ncbi.nlm.nih.gov/12445284/)
35. Kapanadze T, Gamrekelashvili J, Ma C, Chan C, Zhao F, Hewitt S, et al. Regulation of accumulation and function of myeloid derived suppressor cells in different murine models of hepatocellular carcinoma. *J Hepatol.* 2013; 59: 1007–1013. doi: [10.1016/j.jhep.2013.06.010](https://doi.org/10.1016/j.jhep.2013.06.010) PMID: [23796475](https://pubmed.ncbi.nlm.nih.gov/23796475/)
36. Ma S, Cheng Q, Cai Y, Gong H, Wu Y, Yu X, et al. IL-17A produced by $\gamma\delta$ T cells promotes tumor growth in hepatocellular carcinoma. *Cancer Res.* 2014; 74: 1969–1982. doi: [10.1158/0008-5472.CAN-13-2534](https://doi.org/10.1158/0008-5472.CAN-13-2534) PMID: [24525743](https://pubmed.ncbi.nlm.nih.gov/24525743/)
37. Huang B, Lei Z, Zhao J, Gong W, Liu J, Chen Z, et al. CCL2/CCR2 pathway mediates recruitment of myeloid suppressor cells to cancers. *Cancer Lett.* 2007; 252: 86–92. PMID: [17257744](https://pubmed.ncbi.nlm.nih.gov/17257744/)
38. Boelte KC, Gordy LE, Joyce S, Thompson MA, Yang L, Lin PC. Rgs2 mediates pro-angiogenic function of myeloid derived suppressor cells in the tumor microenvironment via upregulation of MCP-1. *PLoS One.* 2011; 6: e18534. doi: [10.1371/journal.pone.0018534](https://doi.org/10.1371/journal.pone.0018534) PMID: [21494556](https://pubmed.ncbi.nlm.nih.gov/21494556/)
39. Hale M, Itani F, Buchta CM, Wald G, Bing M, Norian LA. Obesity triggers enhanced MDSC accumulation in murine renal tumors via elevated local production of CCL2. *PLoS One.* 2015; 10: e0118784. doi: [10.1371/journal.pone.0118784](https://doi.org/10.1371/journal.pone.0118784) PMID: [25769110](https://pubmed.ncbi.nlm.nih.gov/25769110/)
40. Pollard JW. Role of colony-stimulating factor-1 in reproduction and development. *Mol Reprod Dev.* 1997; 46: 54–61. PMID: [8981364](https://pubmed.ncbi.nlm.nih.gov/8981364/)
41. Mok S, Koya RC, Tsui C, Xu J, Robert L, Wu L, et al. Inhibition of CSF-1 receptor improves the antitumor efficacy of adoptive cell transfer immunotherapy. *Cancer Res.* 2014; 74: 153–161. doi: [10.1158/0008-5472.CAN-13-1816](https://doi.org/10.1158/0008-5472.CAN-13-1816) PMID: [24247719](https://pubmed.ncbi.nlm.nih.gov/24247719/)
42. Hassan MM, Abdel-Wahab R, Kaseb A, Shalaby A, Phan AT, El-Serag HB, et al. Obesity early in adulthood increases risk but does not affect outcomes of hepatocellular carcinoma. *Gastroenterology.* 2015; 149: 119–129. doi: [10.1053/j.gastro.2015.03.044](https://doi.org/10.1053/j.gastro.2015.03.044) PMID: [25836985](https://pubmed.ncbi.nlm.nih.gov/25836985/)
43. Morosawa T, Kondo Y, Kogure T, Inoue J, Nakagome Y, Kimura O, et al. Disturbance of regulatory T cells, MDSCs and NK cells is involved in NASH and mouse model of NASH. *Hepatology.* 2015; 62 (Suppl 1): 1264A.